Nuclear Instruments and Methods in Physics Research A 1083 (2026) 171137

Contents lists available at ScienceDirect

Nuclear Inst. and Methods in Physics Research, A

journal homepage: www.elsevier.com/locate/nima

Full Length Article

Performance assessment after long-term irradiation of ATLAS Micromegas detectors using 120 GeV muons at the Gamma Irradiation Facility at CERN

V. D'Amico [a,*], F. Vogel [a], T. Alexopoulos [b], O. Biebel [a], F. Fallavollita [c,1], R. Hertenberger [a], G. Iakovidis [d], P. Iengo [e], N. Kanellos [b], C. Kitsaki [b], F. Kolitsi [f,2], S. Kompogiannis [g], E. Kumar [a], I. Mesolongitis [f], A. Peyaud [h,3], G. Sekhniaidze [e], P. Tzanis [b,2]

[a] Fakultät für Physik, Ludwig-Maximilians-Universität München, Germany
[b] National Technical University of Athens, Heroon Polytechniou 9, Zografou, Greece
[c] Institut Für Physik, Universität Mainz, Germany
[d] Physics Department, Brookhaven National Laboratory, Upton NY, USA
[e] INFN Napoli and Università di Napoli, Dipartimento di Fisica, Italy
[f] University of West Attica, Greece
[g] Aristotle University of Thessaloniki, Greece
[h] IRFU, CEA, Université Paris-Saclay, Gif-sur-Yvette, France

ARTICLE INFO

Keywords:
Muon detector
Micromegas
Irradiation
Detector performance

ABSTRACT

The ATLAS muon spectrometer will face an increased particle rate as a result of the increased instantaneous luminosity expected during the High-Luminosity LHC (HL-LHC) upgrade. The HL-LHC will provide a luminosity of $\mathcal{L} = 7.5{\times}10^{34}$ cm^{-2} s^{-1} and 3000 fb^{-1} of integrated luminosity in 10 years, about 9 times more data of the ones so far collected by the ATLAS experiment. Micromegas chambers are used in the New Small Wheel(s), the first forward muon spectrometer station, to provide tracking and triggering at the intense particle rates expected. The detectors are operated with a ternary gas mixture composed of Ar + 5%CO_2 + 2%iC_4H_{10}, providing good high voltage stability and a large pulse height, important for inclined track reconstruction of particles crossing the detector. To ensure the long-term stable operation of the detector during the whole HL-LHC period, and due to the hydrocarbon content in the mixture, an extensive aging campaign has been ongoing since 2021 at the CERN Gamma Irradiation Facility, where spare production chambers are long-term exposed to a 14 TBq ^{137}Cs γ-source, accumulating so far, a charge equivalent to five years of HL-LHC operations under the highest expected background rate. This paper describes the results of the Micromegas chamber performance studies after two years of gamma irradiation and using the SPS/H4 120 GeV muon beams at CERN.

1. Introduction

The High-Luminosity upgrade of the LHC [1] will increase the instantaneous luminosity to the value of $\mathcal{L} = 7.5 \times 10^{34}$ cm^{-2} s^{-1}, resulting in a higher particle rate in the LHC experiments, especially in the forward regions. Micromegas [2,3] chambers have been installed in the New Small Wheel(s) (NSW) [4] of the ATLAS muon spectrometer. They are expected to operate under a high background radiation environment, up to ~30 kHz/cm^2 extrapolating the current rate measurements [5] to the HL-LHC instantaneous luminosity. The ATLAS performance requirements consist of a spatial resolution of about 100 μm per detector layer for the precision muon track reconstruction, and an angular resolution of approximately 1 mrad for the Level-1 trigger track segment reconstruction from the NSW detectors. The performance is required throughout the operation of these detectors in ATLAS, in order to reduce the rate of fake tracks reconstructed and fake segments triggered to be below ATLAS limits. For this reason, a spare ATLAS Micromegas series production chamber, in particular a small module type-1 (SM1) [6,7], has been long-term exposed to a 14 TBq ^{137}Cs γ-source located at the CERN Gamma Irradiation Facility (GIF++) [8]. The purpose is to operate the detector under an equivalent high-radiation to emulate the amount of radiation

* Corresponding author.
E-mail address: V.Damico@physik-uni-muenchen.de (V. D'Amico).
[1] Now at Max-Planck-Institut für Physik (Werner-Heisenberg-Institut), München, Germany.
[2] Now at CERN, Geneva, Switzerland.
[3] Now at CEA, Grenoble, France.

https://doi.org/10.1016/j.nima.2025.171137
Received 25 March 2025; Received in revised form 25 September 2025; Accepted 28 October 2025
Available online 3 November 2025

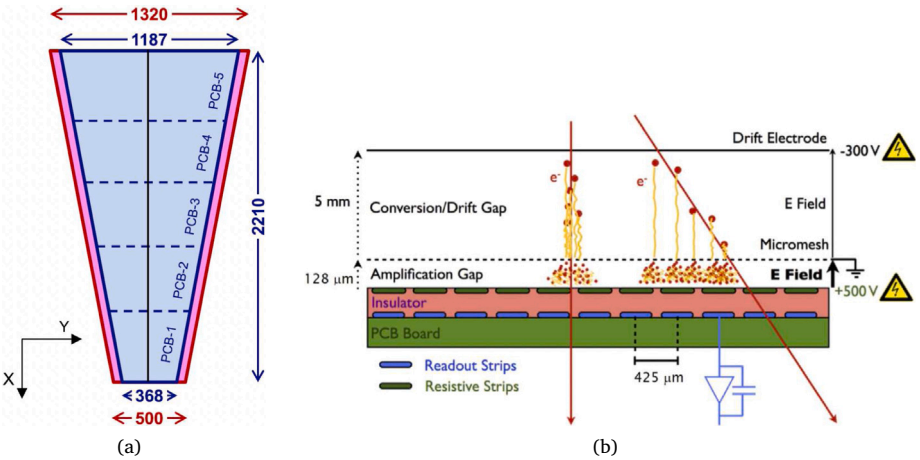

Fig. 1. The shape of a SM1 chamber (a), with in blue the active area of the anodes and in red the full size of the anode panels, including inactive area, with dimensions expressed in mm. The segmentation of the anode plane in five PCBs is also shown, each split in two halves. A scheme of a single Micromegas detector layer (b) with examples of signal production and schematic read-out [6].

background environment expected during HL-LHC operations [9]. The SM1 type Micromegas detectors will be exposed to the largest particle rates during HL-LHC ATLAS muon spectrometer operation due to their close position to the beam pipe. A $120\,\mathrm{GeV}/c$ μ^+ beam from the H4 beam line of the Super Proton Synchrotron (SPS) is used to study the detector performance in the simultaneous presence of beam and background, simulating real detector operation. In this paper the detector performance after more than two years of irradiation is presented.

2. The SM1 Micromegas detector

The SM1 ATLAS Micromegas chamber is a $2\,\mathrm{m}^2$ trapezoidal-shaped Micromegas detector, composed of four active layers. Each layer is segmented into five active 'PCB' sections defined by the size of the Printed Circuit Boards (PCB) of the anode, as shown in Fig. 1(a). Each anode PCB is then segmented into two parts, left and right of the vertical axis of the chamber, which can be supplied with High Voltage (HV) independently. A schematic representation of a single Micromegas layer is shown in Fig. 1(b). It is composed of a cathode and an anode separated by a stainless-steel mesh, creating two gap regions, the drift gap and the amplification gap. The drift cathode is held at a negative voltage of $-240\,\mathrm{V}$ with respect to the mesh, which is grounded and at a distance of 5 mm. The mesh is placed under mechanical tension on top of 128 μm high insulating spacers, separating it from the anode plane, which is composed of resistive strips to which a positive voltage, typically ranging from 490 V to 530 V, is applied. The resistive strips are capacitively coupled to copper readout strips with 425 μm pitch, and connected to the front-end electronics. The gaps are filled with a gas mixture of $\mathrm{Ar} + 5\%\mathrm{CO}_2 + 2\%\mathrm{iC}_4\mathrm{H}_{10}$, flushed at $\sim 30\,\mathrm{Nl/h}$ at atmospheric pressure, as done during ATLAS operation. A charged particle entering the detector ionizes the gas in the drift gap. Due to the electric field, the generated positive ions move towards the cathode, while the electrons move through the mesh to the anode. In the amplification gap, the high electric field of $\sim 40\,\mathrm{kV/cm}$ generates a Townsend avalanche of electrons, amplifying the charge collected by the resistive strips, which induces a signal on the copper strips that is processed by the readout electronics.

3. Irradiation studies

The robustness of the SM1 chamber after several years of operation is evaluated by exposing the detector to long-term irradiation at the GIF++ at CERN. The GIF++ is a $\sim 100\,\mathrm{m}^2$ bunker containing a 14 TBq $^{137}\mathrm{Cs}$ source at its center, producing a uniform background γ-field in the transverse plane, thanks to shaped angular correction Lead filters [10]. The γ-field consists of the primary $662,\mathrm{keV}$ photons and a broad tail of lower-energy scattered photons from the Compton effect, which contribute 54.5% to the total spectrum [10]. The intense flux of $662\,\mathrm{keV}$ photons allows for the accelerated accumulation of doses equivalent to HL-LHC experimental conditions. It is tunable using a set of three shaped lead filters, that can attenuate the flux by a factor 1 up to ∼40000 depending on the combination of the filters used.

The irradiation of the detector started in 2021, and lasted for two years, which is equivalent to several years of the HL-LHC operation. The Micromegas detector was kept at a distance of approximately 1 m from the source. The central area of the detector was positioned exactly in front of the source and at the same height as the muon beam provided by the H4 beam line. The resulting irradiation of the central area is almost uniform. For this reason, all the tests reported in this paper are focused on this central area, corresponding to PCB-3 of the Micromegas detector. Results are scaled, in particular, to the position of the first instrumented strip of PCB-1 that will face the highest particle rate in ATLAS operations. Stable high voltage operation of the detector at 520 V without breakdowns or discharges, during the whole period both with and without irradiation, was observed. Fig. 2 shows the accumulated charge in $\mathrm{C/cm}^2$ of each of the eight high voltage sectors of the benchmark PCB-3 normalized to its area.

An accumulated charge of $0.34\,\mathrm{C/cm}^2$ is, according to our present knowledge [11], equivalent to five years of HL-LHC operations at 520 V for the first strip of the PCB-1, the one with the largest expected particle rate of $\sim 30\,\mathrm{kHz/cm}^2$. In these calculations, ATLAS measurements are extrapolated to the HL-LHC expectations with no safety factor applied. Due to the approximately quadratic decrease of the particle rate with the radial distance from the beam axis, as observed in the first runs in ATLAS, an accumulated charge of $0.29\,\mathrm{C/cm}^2$ is equivalent to 10 years of HL-LHC operations at 520 V for the last strip of PCB-1, which will have a lower particle rate and will therefore accumulate less charge.

4. Test beam results

Several test beams were performed using the SPS H4 beam line during the irradiation campaign at GIF++ to validate and investigate the performance of the irradiated detector over time. In particular, the results reported in this paper are evaluated after approximately two years of irradiation and the accumulation of more than $0.2\,\mathrm{C/cm}^2$ for all the detector layers as shown in Fig. 2, during a test beam conducted in July 2023.

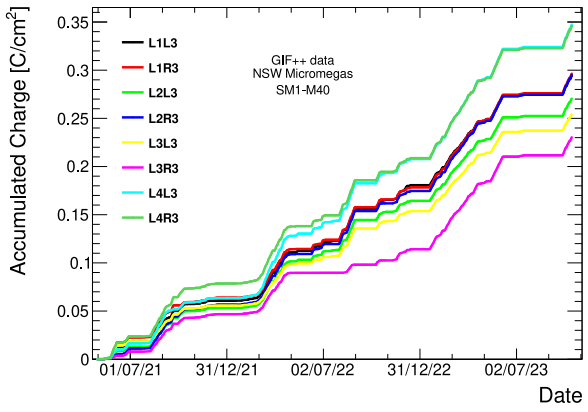

Fig. 2. Accumulated charge over time normalized to the active area of the high voltage sector, where the displayed lines belong to the left and right halves of the benchmark PCB-3, xxL3 and xxR3, and for the 4 layers, L1xx through L4xx of the SM1-M40 Micromegas detector. The total accumulated charge is different among sectors due to different intrinsic gain of the layers, different exposure to the source, or periods with lower or switched off HV.

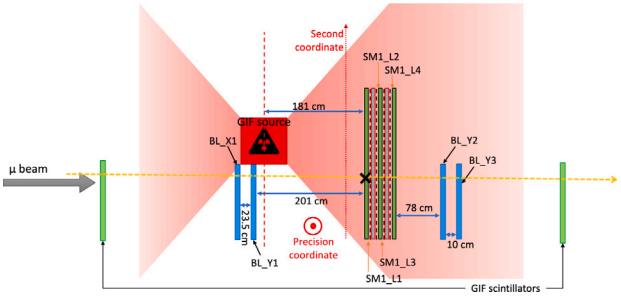

Fig. 3. Schematic of the experimental setup used in the test beam (not to scale). The distances between the SM1 chamber and the tracking detectors are given. BL_X1 and BL_Y1 tracking chambers are positioned outside of the irradiation cone of the source.

4.1. Experimental setup and data reconstruction

The test beam experimental setup consisted of the SM1-M40 detector placed 181 cm away from the GIF++ source, with layer-1 facing the source, and four one-dimensional $40\times40\,\mathrm{cm}^2$ Micromegas chambers (BL_X1, BL_Y1, BL_Y2, BL_Y3) providing precision reference tracking. The greater distance of the detector from the GIF++ source, compared to the irradiation distance, was needed to ensure that it was both in the irradiation cone of the source and on the path of the H4 muon beam. A schematic of the experimental setup used is shown in Fig. 3.

A trigger was provided by a coincidence of two scintillators from the GIF++, placed upstream and downstream outside the facility, shielded from the source. The Micromegas chambers were instrumented with the ATLAS Micromegas electronics, consisting of front-end boards equipped with VMM3a ASICs [12,13]. Only PCB-3 of the SM1 detector was instrumented, as it was the fully irradiated one and was centered at the correct beam height. Data were collected both in perpendicular and 29° inclined configuration of the chamber with respect to the μ-beam axis. The cathode voltage was set to −240 V for all the chambers, while the anode voltage was scanned from 490 V to 530 V on the SM1 detector. The reference detectors had a fixed anode voltage of 510 V, which was found to be a good working point for these chambers having a good efficiency and amplification gain for perpendicular muons. Only events with a single well reconstructed track in the BL tracking chambers and a single cluster in BL_X1 and BL_Y1 chambers were analyzed, consisting of about 30 000–80 000 analyzed events for each data point depending on the background intensity. Randomly

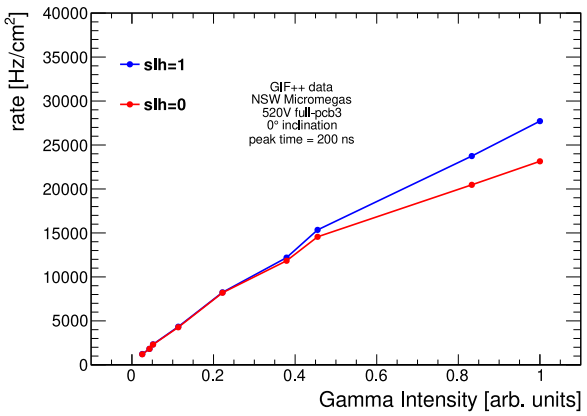

Fig. 4. Cluster rate normalized to the active area of the benchmark PCB-3 as a function to the intensity of the GIF++ source, where Gamma Intensity 1 corresponds to no GIF++ source attenuation, when the source is not attenuated by any filter. The two lines show the different settings of the *slh* parameter [14] of the VMM electronics, corresponding to a higher ($slh = 1$) or lower ($slh = 0$) bias current at the input of the electronic channels.

triggered events without μ-beam and γ-irradiation were taken to set the charge thresholds to be applied in the data taking to remove baseline fluctuations from the measured strip signal. The time of the signal is determined for each channel from the VMM3a ASIC, and calibrated for each channel individually. In addition, the time of the trigger is recorded and applied as a global t_0 in the computation of the strip time. A group of nearby responding channels is identified as a cluster, and the position coordinate on the layer is measured as the cluster charge-centroid, computed by weighting the position of each channel with its charge with the formula: $x_q = \Sigma_i\ q_i X_i / \Sigma_i\ q_i$.

4.2. Rate measurement

The incident background particle rate was measured using a random trigger and recording accidental events with only photons from the source and no μ beam. The intensity of the source was tuned by adjusting various filter settings to obtain different photon fluxes and therefore varying background rates. The cluster rate was determined from the mean number of reconstructed clusters per event, divided by the time acquisition window of 200 ns, and normalized to the active area of the detector. As shown in Fig. 4, the expected linear scaling of the rate as a function of the photon intensity is observed up to $10\,\mathrm{kHz/cm}^2$. Beyond this point, the probability of overlapping signals increases, leading to a saturation of the readout electronics.

This saturation is expressed in data loss caused by multiple signals per strip within the acquisition window and the dead time of the VMM channel. To minimize the data loss, adjustments to the VMM's operational parameters, particularly to the slh parameter, contained in the global registers were made [14]. This register increases the feedback current in the shaper to compensate for the input current after the detection of a signal. As a result, the shaper goes below threshold faster, reducing the channel dead time. Previously missing strips are recovered increasing the performance at high background rates. With this configuration, the saturation effect is expected to impact only on a few strips of the detector in the most strongly irradiated area during HL-LHC operations.

4.3. Spatial resolution

Measurements of the spatial resolution of the SM1 layers were performed along the precision coordinate for both perpendicular and inclined setup configuration. The resolution was calculated based on

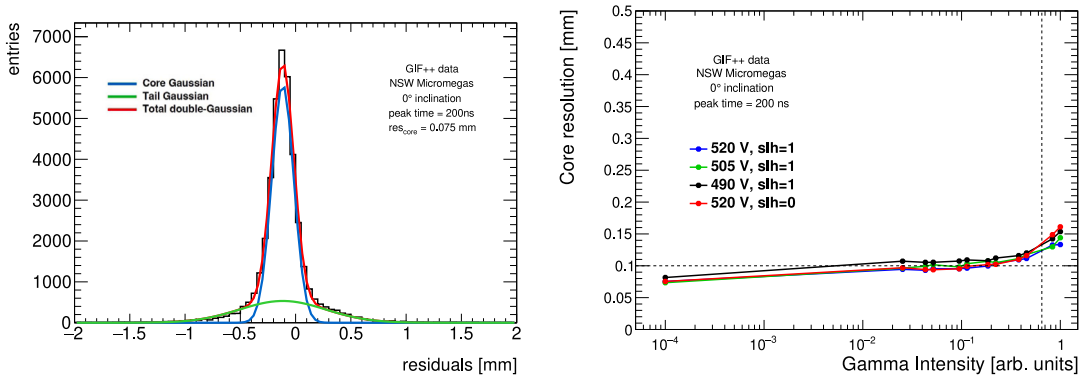

(a) (b)

Fig. 5. Shown is the spatial core resolution for perpendicular tracks: in no background conditions (a) and as a function of the intensity of the γ-irradiation (b). The value Gamma intensity = 10^{-4} means γ-source OFF. The applied anode voltage was set to 520 V and the peak time, i.e. the integration time used to detect the peak signal and calculate the charge within that time interval [12], was set to 200 ns. The small shift in the residuals distribution (a) is due to a residual misalignment of the detector layer, not influencing the resolution measurement.

the difference between the track prediction of the position and the reconstructed cluster position, commonly referred to as the residuum or residual. This evaluation was done after applying software-based alignment corrections in order to remove the effects of shifts and rotations between the reference chambers and the SM1 layers. The residual distribution for layer-1 with perpendicular tracks and without background coming from the gamma source is shown in Fig. 5(a).

The spatial resolution is obtained by performing a double-Gaussian fit on the residual distribution. The narrower, core Gaussian accounts for the intrinsic resolution, while the broader, tail Gaussian also accounts for broadening effects such as multiple scattering or delta-electrons. The resolution of the reference track, which was measured to be 60 μm, was subtracted in quadrature from the Standard deviation of the core Gaussian to compute the spatial resolution of the detector. The core spatial resolution was found to be 75 μm for layer-1, with the other layers showing similar values below 100 μm. The spatial resolution was also evaluated in presence of photon background coming from the GIF++ source, and is summarized in Fig. 5(b), showing an almost constant spatial resolution, with a value of about 100 μm as a function of the intensity of the background radiation (*Gamma Intensity*). Only at the highest intensities of the source, the resolution degrades, reaching ∼150 μm. A *Gamma Intensity* of ∼0.65 corresponds to the background intensity expected for the most strongly irradiated regions in the ATLAS forward muon spectrometer closest to the beam-pipe at HL-LHC. A resolution of ∼100 μm is satisfied by the Micromegas detectors even at the highest background rates expected in ATLAS HL-LHC operation. The anode voltage was scanned from 490 V to 520 V, and from Fig. 5(b) a 10% difference in the spatial resolution at 490 V, due to the lower amplification gain and the consequently worse cluster reconstruction is visible. Also, the $sIh = 0$ parameter was tested, yielding similar resolutions up to the largest background intensities, at which the performance is impacted by the data loss due to the front-end electronics.

For the data taken with the inclined setup configuration the cluster position is reconstructed differently. The cluster-time corrected centroid method [15] is applied in this case, for which the charge centroid position is corrected by exploiting the correlation between the residuals distribution and the cluster time distribution, defined as the charge-weighted average of the times of the strips forming the cluster. In this method, the time information is of crucial importance and a fine-tuned calibration of the times registered by the electronic channels is fundamental. Such time calibration was performed with a set of data with only muon hits, exploiting the integrated distributions of the times for each individual channel. The times detected by the electronic channels were aligned, setting an individual t_0^i offset for each electronic channel. The registered time of the trigger signal for each event was also applied as an additional global t_0 offset, equal for all the channels. Detector shifts and rotations were corrected again for the inclined setup configuration, in order to account for additional misalignments caused by the movement of the detector. Also in this case, the spatial residual distribution between the cluster-time corrected centroid reconstructed cluster position and the extrapolated track position was evaluated as a function of the intensity of the GIF++ source. A double Gaussian fit was performed on the residual distribution, obtaining a core resolution of 151 μm for layer-1 with no background. This result, thanks to the refinement of the reconstruction and the fine tuning of the alignment and time calibration performed in this work, is the best ever obtained for the spatial resolution of a full-size ATLAS Micromegas detector tilted by 29°. The results of the spatial resolution for 29° inclined tracks are summarized in Fig. 6, showing a slight degradation of the resolution with higher background intensities, with values reaching 210 μm at the maximum intensity of the source.

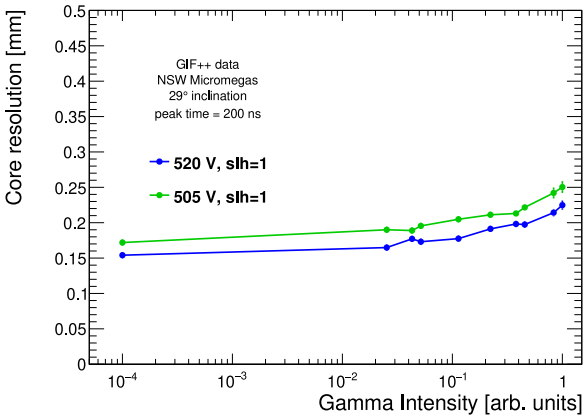

Fig. 6. Shown is the spatial core resolution for 29° inclined tracks, as a function of the intensity of the γ-irradiation. The value Gamma intensity = 10^{-4} means γ-source OFF.

The expected background conditions of the detector with this inclination in HL-LHC operations, correspond to a low intensity of the source (Gamma Intensity $< 10^{-2}$), where the measured resolution is smaller than 160 μm. A second measurement with reduced amplification voltage of 505 V was performed to measure the spatial resolution in case of operation of the detector with reduced gain in the experiment, resulting in a ∼15% difference in the spatial resolution, as visible in Fig. 6. This slightly poorer resolution is the result of a lower strip charge due

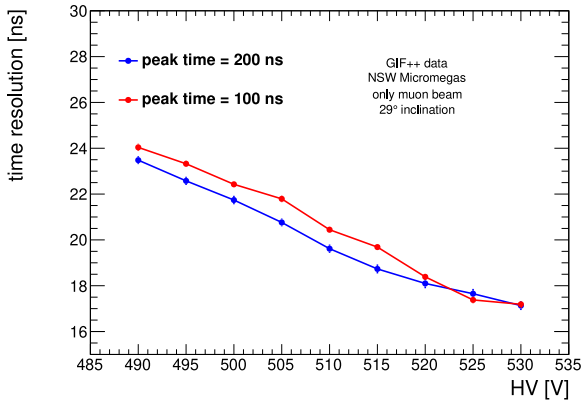

Fig. 7. Shown is the time resolution as a function of the anode voltage, for two values of the peaking time: 200 ns or 100 ns. The resolution is evaluated from the weighted sigma of a double Gaussian fit to the time difference distribution of earliest strips of back-to-back clusters in the first two layers of the detector. Data with only muon beam and no photon background from the GIF++ source were used.

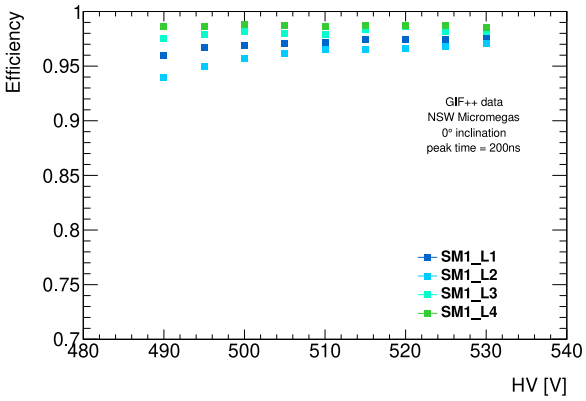

Fig. 8. Shown is the single plane detector efficiency without irradiation as a function of the anode amplification voltage for all four layers of the SM1 detector, in the perpendicular setup configuration. The differences between layers are due to different intrinsic gain of the layer by construction, as for instance due to a different pillar height.

to the lower gas gain, which results in, on average, a smaller cluster size compared to the optimal 6 strips clusters for 29° inclined tracks, worsening the precision of the cluster position reconstruction.

4.4. Time resolution

The time resolution was studied to determine the timing performance of the detector, important for the improvement of the reconstruction performance of inclined tracks and for the reduction of the trigger time spread during ATLAS operation. For this study data sets with only muons and no background from the source were used. Clusters in the first two layers of the SM1 detector closest in position, defined as back-to-back clusters were compared. The distribution of the time differences of the earliest strips in the two back-to-back clusters were fitted with a double-Gaussian function. The resolution is calculated from the core and the tail Gaussian, weighting for the integral of each of the two functions and dividing by $\sqrt{2}$, assuming that the planes have the same time resolution. The results obtained for the time resolution as a function of the anode amplification voltage of the detector are shown in Fig. 7. The results are reported for two configurations of the electronics, in particular for two values of the peaking time, that refers to the integration time used to detect the peak signal and calculate the charge within that time interval [12].

The time resolution improves with higher gain, from ∼21 ns at 505 V to ∼17 ns at 530 V for 200 ns peaking time. The 100 ns peaking time results show a similar trend with a slightly worse time resolution at a lower gain. The reason is the lower charge collected on the strips and the worse time measurement obtained by the electronics in this reduced time interval [13]. Both time resolution results are compatible at higher gains, above 520 V. The method used here for the measurement of the time resolution does not consider the drift time difference between the two clusters, which can result in a smearing of the time distribution.

4.5. Efficiency

The efficiency as a function of the anode amplification voltage is shown in Fig. 8 for all four layers of PCB-3, scanning the voltage from 490 V up to 530 V. For this study, data with only muon beam and no background coming from the GIF++ source were used. Efficiencies between 96% and 99% were reached on all layers at anode voltages above 505 V. These results demonstrate the high gain that is provided by the $Ar+5\%CO_2+2\%iC_4H_{10}$ gas mixture, in particular using 2% of isobutane, and the excellent performance and stability of the Micromegas detector.

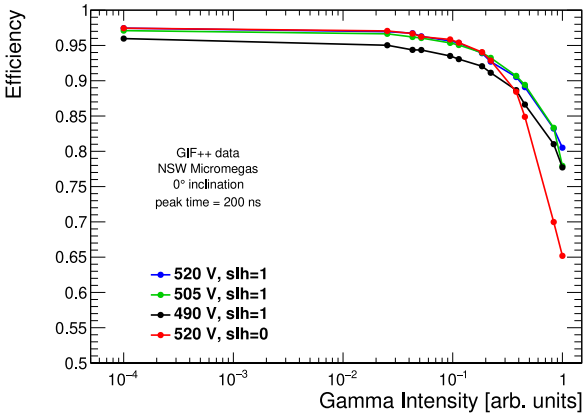

Fig. 9. Shown is the detector layer-1 efficiency as a function of the intensity of the γ-irradiation, in the perpendicular setup configuration. The value Gamma intensity = 10^{-4} means γ-source OFF.

The efficiency of the SM1 detector was also studied as a function of the *Gamma Intensity*, modulating with the filters the irradiation from the GIF++ source. Starting from tracks reconstructed with the external chambers, for each layer of the SM1 detector a one-dimensional interval of ±2 mm around the extrapolated position was defined. The efficiency is defined as the ratio between the number of tracks with at least one cluster in the interval and the total number of reference tracks. In Fig. 9 the efficiency as a function of the intensity of the source is shown for layer-1. A drop of the efficiency for increasing photon background intensity is visible. Especially at the highest intensities the single-plane efficiency drops from ∼97% to below 80%, where the performance is impacted by the data loss due to the front-end electronics. The drop is similar for the three values of the anode voltage tested (520 V, 505 V, and 490 V), with an almost constant 2% efficiency difference for the lower gain points at 490 V ($sIh = 1$). Also, the $sIh = 0$ parameter was tested, obtaining similar single-plane efficiencies at the voltage of 520 V up to intermediate background intensities, and with a larger efficiency drop visible at the largest background intensities, as expected from the rate drop shown in Fig. 4. Increasing the bias current at the input node, setting the VMM sIh parameter to 1, up to 15% single-plane efficiency can be recovered as visible from Fig. 9.

In particular, it has been measured that a Gamma Intensity of ∼0.65 corresponds to the background intensity expected for the most strongly irradiated region in the ATLAS forward muon spectrometer closest to

the beam pipe at HL-LHC. As a result, a single-plane efficiency of ∼85% is expected for the innermost strips of the ATLAS Micromegas chambers under those conditions. Efficiencies larger than 90% and 95% are instead expected for the rest of the PCB-1 and the other PCBs of the detector, respectively, during HL-LHC operations.

5. Conclusion

A full-size series production SM1 ATLAS Micromegas chamber has been long-term exposed to an intense photon source at the CERN GIF++ since 2021. The GIF++ has provided a powerful opportunity to accumulate charges equivalent to several years of HL-LHC operations in two years of irradiation. An equivalent charge of about five years of operation under the highest HL-LHC expected background rate has been accumulated by the detector, which has shown a very good high voltage stability, both with and without irradiation, at constant anode currents during irradiation. Detector stability and performance after long-term irradiation and in conditions with HL-LHC expected background particle rates in the end-cap muon spectrometer of the ATLAS experiment were investigated. The muon reconstruction performance has been validated exploiting 120 GeV/c muons of the SPS H4 muon beam line, and the simultaneous intense background provided by the GIF++ photon source. A spatial resolution better than 100 μm has been measured for perpendicular tracks. Values of 100 μm were achieved at highest background rates as expected for this detector under HL-LHC operations.

Excellent spatial resolution results for a full-size Micromegas detector have been also observed for μ traversing the detector under 29° of inclination. A spatial resolution of 151 μm has been measured in no background conditions. The result has been obtained thanks to the use of the cluster-time corrected centroid method for cluster position reconstruction, along with the fine tuning of the alignment and the time calibration presented in this work. A very high single plane efficiency above 95% has been measured for perpendicular tracks at the nominal anode amplification voltage value of 520 V. However, an efficiency drop has been observed for high γ-intensities, where the performance is impacted by the data loss due to the front-end electronics saturation effect. This issue has been mitigated by using a larger bias current of the VMM channels, set through the $slh = 1$ parameter configuration, allowing the partial recovery of the hit rate and thus the detection efficiency at high background rates.

The time resolution of the detector was measured as 18 ns for an amplification voltage of $V_{amp} = 520$ V.

In summary, the robustness of the ATLAS Micromegas detectors has been validated under intense background fluxes equivalent to several years of HL-LHC operations. The overall detector performance has been observed to be unaffected by the accumulated irradiation, resulting in nominal design resolutions, high gain and no sign of decrease in performance.

CRediT authorship contribution statement

V. D'Amico: Writing – review & editing, Writing – original draft, Validation, Software, Project administration, Methodology, Investigation, Formal analysis, Data curation. **F. Vogel:** Writing – review & editing, Validation, Software, Methodology, Investigation, Formal analysis, Data curation. **T. Alexopoulos:** Writing – review & editing, Supervision, Project administration, Methodology, Funding acquisition, Data curation, Conceptualization. **O. Biebel:** Writing – review & editing, Supervision, Resources, Funding acquisition. **F. Fallavollita:** Project administration, Investigation, Data curation. **R. Hertenberger:** Writing – review & editing, Validation, Supervision, Project administration, Methodology, Investigation, Conceptualization. **G. Iakovidis:** Writing – review & editing, Validation, Methodology. **P. Iengo:** Writing – review & editing, Supervision, Project administration, Funding acquisition, Conceptualization. **N. Kanellos:** Software, Methodology, Investigation, Data curation. **C. Kitsaki:** Methodology, Investigation, Formal analysis, Data curation. **F. Kolitsi:** Software, Methodology, Investigation, Formal analysis, Data curation. **S. Kompogiannis:** Resources, Project administration. **E. Kumar:** Methodology, Investigation, Formal analysis, Data curation. **I. Mesolongitis:** Software, Resources, Data curation. **A. Peyaud:** Conceptualization. **G. Sekhniaidze:** Resources, Project administration. **P. Tzanis:** Software, Investigation, Data curation.

Declaration of competing interest

The authors declare the following financial interests/personal relationships which may be considered as potential competing interests: Otmar Biebel reports financial support was provided by Federal Ministry of Education and Research Berlin Office. Eshita Kumar reports financial support was provided by Federal Ministry of Education and Research Berlin Office. Ralf Hertenberger reports financial support was provided by Federal Ministry of Educaton and Research Berlin Office. Valerio D'Amico reports financial support was provided by Federal Ministry of Education and Research Berlin Office. Fabian Vogel reports financial support was provided by Federal Ministry of Education and Research Berlin Office. George Iakovidis reports financial support was provided by US Department of Energy. If there are other authors, they declare that they have no known competing financial interests or personal relationships that could have appeared to influence the work reported in this paper.

Acknowledgments

This work was supported by the German Federal Ministry of Education and Research (BMBF) within the framework program "Exploration of the Universe and Matter (ErUM)" [FSP-ATLAS]; the Hellenic Basic Research Program PEVE2021 of the National Technical University of Athens; the ATLAS Collaboration and ATLAS Muon Spectrometer collaboration. This work was funded in part by the U.S. Department of Energy, Office of Science, United States, High Energy Physics, United States under Contracts DE-SC0012704. We would also like to thank the GIF++ for the support in the operations and organization of irradiation and beam times, and Markus Joos and the Beamline for Schools (BL4S) CERN program for providing us the four $40 \times 40\,\mathrm{cm}^2$ Micromegas chambers used in the test beam as reference tracking chambers. Finally, a special thanks to Christoph Jagfeld for his useful advice for the data analysis optimization.

Data availability

Data will be made available on request.

References

[1] L. Rossi, O. Brüning, High luminosity large hadron collider: A description for the European strategy preparatory group, 2012, CERN-ATS-2012-236.
[2] Y. Giomataris, Ph. Rebourgeard, J.P. Robert, G. Charpak, MICROMEGAS: a high-granularity position-sensitive gaseous detector for high particle-flux environments, Nucl. Instrum. Methods A 376 (1996) 29–35.
[3] T. Alexopoulos, et al., A spark-resistant bulk-micromegas chamber for high-rate applications, Nucl. Instr. Methods A 640 (2011) 110–118.
[4] The ATLAS collaboration, New small wheel technical design report, 2013, CERN-LHCC-2013-006.
[5] The ATLAS collaboration, NSW MicroMegas cluster rates, 2024, ATLAS Muon Spectrometer Plots MDET-2024-01.
[6] T. Alexopoulos, et al., Construction techniques and performances of a full-size prototype micromegas chamber for the ATLAS muon spectrometer upgrade, Nucl. Instrum. Methods A 955 (2020) 162086.
[7] J. Agarwala, et al., Construction and test of the SM1 type micromegas chambers for the upgrade of the ATLAS forward muon spectrometer, Nucl. Instrum. Methods A 1040 (2022) 167285.
[8] M.R. Jaekel, et al., CERN GIF++ : A new irradiation facility to test large-area particle detectors for the high-luminosity LHC program, 2014, PoS (TIPP2014) 102.

[9] F. Vogel, Test of ATLAS micromegas detectors with ternary gas mixture at the CERN gif++ facility, 2022, PoS (EPS-HEP2021) 757.
[10] D. Pfeiffer, et al., The radiation field in the Gamma irradiation facility GIF++ at CERN, Nucl. Instrum. Methods A 866 (2017) 91–103.
[11] F. Vogel, Long-Term Irradiation Studies of Large-Area Micromegas Detectors for the ATLAS NSW Upgrade (Ph.D. thesis), 2024.
[12] G. Iakovidis, et al., The new small wheel electronics, J. Instrum. 18 (2023) P05012.
[13] G. de Geronimo, G. Iakovidis, S. Martoiu, V. Polychronakos, The VMM3a ASIC, 2022, IEEE Trans. Nucl. Sci. 69 (2022) 4, 976-985.
[14] The ATLAS collaboration, The VMM3a user's guide, 2022, ATL-MUON-PUB-2022-002.
[15] B. Flierl, Particle Tracking with Micro-Pattern Gaseous Detectors (Ph.D. thesis), 2018.